# Supplementary material for *Ab initio* structure modeling of complex thin-film oxides: thermodynamical stability of TiC/thin-film alumina (Rohrer *et al* 2009 *J. Phys.: Condens. Matter* 22 015004)

**J Rohrer[1], C Ruberto[1,2] and P Hyldgaard[1]**

[1] BioNano Systems Laboratory, Department of Microtechnology, MC2, Chalmers University of Technology, SE-412 96 Gothenburg
[2] Materials and Surface Theory Group, Department of Applied Physics, Chalmers University of Technology, SE-412 96 Gothenburg

E-mail: rohrer@chalmers.se

This document contains supplementary material for the paper '*Ab-initio* structure modeling of complex thin-film oxides: thermodynamical stability of TiC/thin-film alumina', Rohrer *et al* 2009 *J. Phys.: Condens. Matter* **22** 015004

## 1. Supplementary material for Section 3.3.

Tables 1, 2, and 3 list the stacking sequences of all unrelaxed thin-film candidates. The main steps of the procedure for identifying these sequences is described in the research paper. Here, we add some details that are concerned with the choice of the surfaces of the films.

For $Al_{4n}O_{6n}$ or $Al_{4n-4}O_{6n}$ thin-film geometries, the surface is terminated by two Al pairs (per cell) or by a full O layer. In both cases, the surface structures are fully determined by truncating the alumina bulk stacking sequences of Table II in the research paper. For $Al_{4n-4}O_{6n}$, the surface is terminated by one Al pair per cell.

Thus, in the case of $\kappa$-derived films, there two possible surface terminations for each sequence; one given by removing the first Al pair at the surface, one given by removing the second Al pair at the surface. For example the truncated sequence $Ab_\gamma c_\beta Bc_\alpha c_\gamma$ yields the two possibilities $Ab_\gamma c_\beta Bc_\alpha$ and $Ab_\gamma c_\beta Bc_\gamma$. Hence, the number of $Al_{4n-2}O_{6n}$ films is double as high as the number of $Al_{4n}O_{6n}$ or $Al_{4n-4}O_{6n}$ films.

In the case of an $\alpha$-derived film, we have, for example, the truncated sequence $Ac_2c_3Bc_1c_2$, yielding $Ac_2c_3Bc_1$ or $Ac_2c_3Bc_2$. However, in the second possible $Al_{4n-2}O_{6n}$ sequence, $Ac_2c_3Bc_2$, the Al pair in the second Al layer is directly on top of an Al pair in the layer below. This is electrostatically unfavorable, as we have explicitly confirmed by total energy calculations for a few cases for initial geometries of the type $Ac_2c_3Bc_2$, and we therefore do, in general, not consider such geometries as possible starting configurations.

| alumina group | $Al_4O_{12}$ films: alumina stacking | $Al_4O_{12}$ films: coord. of Al ions | $Al_4O_{12}$ films: $E_{rel}$ (eV/cell) | $Al_8O_{18}$ films: alumina stacking | $Al_8O_{18}$ films: coord. of Al ions | $Al_8O_{18}$ films: $E_{rel}$ (eV/cell) | $Al_{12}O_{24}$ films: alumina stacking | $Al_{12}O_{24}$ films: coord. of Al ions | $Al_{12}O_{24}$ films: $E_{rel}$ (eV/cell) |
|---|---|---|---|---|---|---|---|---|---|
| $\alpha$ | $Ac_3c_2B$ | $OO$ | 0.71 | $Ac_3c_2Bc_1c_3A$ | $OO:OO$ | 5.02 | $Ac_3c_2Bc_1c_3Ac_2c_1B$ | $OO:OO:OO$ | 2.34 |
| $\alpha$ | $Ab_2b_3C$ | $OO$ | 0.72 | $Ab_2b_3Cb_1b_2A$ | $OO:OO$ | 2.78 | $Ab_2b_1Cb_1b_2Ab_3b_1C$ | $OO:OO:OO$ | 2.19 |
| $\kappa[001]$ | $Ab_\gamma c_\beta B$ | $T_\uparrow O$ | 8.02 | $Ab_\gamma c_\beta Bc_\alpha c_\gamma A$ | $T_\uparrow O:OO$ | 9.03 | $Ab_\gamma c_\beta Bc_\alpha c_\gamma Ac_\beta b_\gamma C$ | $T_\uparrow O:OO:T_\uparrow O$ | 7.15 |
| $\kappa[001]$ | $\underline{Ab_\gamma c_\beta C}$ | $T_\uparrow O$ | $\underline{0.01}$ | $Ac_\beta b_\gamma Cb_\alpha b_\beta A$ | $T_\uparrow O:OO$ | 2.46 | $Ac_\beta b_\gamma Cb_\alpha b_\beta Ab_\gamma c_\beta B$ | $T_\uparrow O:OO:T_\uparrow O$ | 7.26 |
| $\kappa[001]$ | $Ac_\alpha c_\beta B$ | $OO$ | 4.43 | $Ac_\alpha c_\beta Bc_\gamma a_\beta C$ | $OO:T_\uparrow O$ | 2.03 | $Ac_\alpha c_\beta Bc_\gamma a_\beta Ca_\alpha a_\gamma B$ | $OO:T_\uparrow O:OO$ | 4.05 |
| $\kappa[001]$ | $Ab_\alpha b_\gamma C$ | $OO$ | 2.43 | $Ab_\alpha b_\gamma Cb_\beta a_\gamma B$ | $OO:T_\uparrow O$ | 1.39 | $Ab_\alpha b_\gamma Cb_\beta a_\gamma Ba_\alpha a_\beta C$ | $OO:T_\uparrow O:OO$ | 3.55 |
| $\kappa[00\bar{1}]$ | $\underline{Ac_\gamma a_\beta B}$ | $OT_\downarrow$ | $\underline{0.20}$ | $Ac_\gamma a_\beta Ba_\gamma a_\alpha C$ | $OT_\downarrow:OO$ | 2.69 | $Ac_\gamma a_\beta Ba_\gamma a_\alpha Ca_\beta c_\gamma B$ | $OT_\downarrow:OO:OT_\downarrow$ | 5.37 |
| $\kappa[00\bar{1}]$ | $\underline{Ab_\beta a_\gamma C}$ | $OT_\downarrow$ | $\underline{0.00}$ | $\underline{Ab_\beta a_\gamma Ca_\beta a_\alpha B}$ | $OT_\downarrow:OO$ | $\underline{0.00}$ | $Ab_\beta a_\gamma Ca_\beta a_\alpha Ba_\gamma b_\beta C$ | $OT_\downarrow O:OO:OT_\downarrow$ | 4.15 |
| $\kappa[00\bar{1}]$ | $Ac_\gamma c_\alpha B$ | $OO$ | 4.43 | $Ac_\gamma c_\alpha Bc_\beta b_\gamma A$ | $OO:OT_\downarrow$ | 2.79 | $\underline{Ac_\gamma c_\alpha Bc_\beta b_\gamma Ab_\beta b_\alpha C}$ | $OO:OT_\downarrow:OO$ | $\underline{0.12}$ |
| $\kappa[00\bar{1}]$ | $Ab_\beta b_\alpha C$ | $OO$ | 2.43 | $Ab_\beta b_\alpha Cb_\gamma c_\beta A$ | $OO:OT_\downarrow$ | 1.48 | $\underline{Ab_\beta b_\alpha Cb_\gamma c_\beta Ac_\gamma c_\alpha B}$ | $OO:OT_\downarrow:OO$ | $\underline{0.00}$ |

**Table 1.** Stacking sequence and Al coordination [$O$ for octahedral, $T$ for tetrahedral, with the arrow indicating the direction in which each tetrahedron vertex is pointing: towards the film surface ($\uparrow$) or towards the TiC/film interface ($\downarrow$)] of *unrelaxed* alumina films with $Al_{4n-4}O_{6n}$ stoichiometry and their total energies $E_{rel}$ *after* relaxation (given relative to the structure with lowest total energy for each film thickness). The configurations are grouped together according to the phase and orientation of the alumina bulk structures from which they are derived (left column). Configurations that differ only by a rotation of 180° around TiC[111] are organized into subgroups separated by larger whitespace. In general, the unrelaxed and relaxed atomic structures differ considerably. The stable and potentially metastable (see research paper for details) configurations are underlined. The *ab initio* study and comparison permit us to make the following set of observations: (i) The unrelaxed configurations with an $AC$ stacking in the first two O layers yield relaxed structures that are in general more favorable than those obtained from configurations in which the stacking sequence has been rotated by 180° around TiC[111] ($AB$ O stacking); (ii) While for the $Al_4O_{12}$ films two different unrelaxed structures lead to the stable configuration, for the other two film thicknesses only one structure leads to the stable configuration; (iii) In general, the stable configurations are obtained from TiC[111]/$\kappa[00\bar{1}]$ initial structures; (iv) The $\alpha$-type films lead to neither stable nor metastable configurations; and (v) While the stable $Al_4O_{12}$ and $Al_8O_{18}$ films are both obtained from the same unrelaxed interface sequence (same line), the stable $Al_{12}O_{24}$ film derives from another interface sequence.

| alumina group | $Al_6O_{12}$ films: alumina stacking | coord. of Al ions | $E_{rel}$ (eV/cell) | $Al_{10}O_{18}$ films: alumina stacking | coord. of Al ions | $E_{rel}$ (eV/cell) | $Al_{14}O_{24}$ films: alumina stacking | coord. of Al ions | $E_{rel}$ (eV/cell) |
|---|---|---|---|---|---|---|---|---|---|
| $\alpha$ | $Ac_3c_2Bc_1$ | $OO:O$ | 0.78 | $\underline{Ac_3c_2Bc_1c_3Ac_2}$ | $OO:OO:O$ | 0.15 | $Ac_3c_2Bc_1c_3Ac_2c_1Bc_3$ | $OO:OO:OO:O$ | 0.99 |
| $\alpha$ | $\underline{Ab_2b_3Cb_1}$ | $OO:O$ | 0.02 | $\overline{Ab_2b_3Cb_1b_2Ab_3}$ | $OO:OO:O$ | 3.22 | $Ab_2b_3Cb_1b_2Ab_3b_1Cb_2$ | $OO:OO:OO:O$ | 0.97 |
| $\kappa[001]$ | $Ab_\gamma c_\beta Bc_\alpha$ | $T_\uparrow O:O$ | 0.77 | $Ab_\gamma c_\beta Bc_\alpha c_\gamma Ab_\gamma$ | $T_\uparrow O:OO:O$ | 1.21 | $Ab_\gamma c_\beta Bc_\alpha c_\gamma Ac_\beta b_\gamma Cb_\alpha$ | $T_\uparrow O:OO:T_\uparrow O:O$ | 2.89 |
| $\kappa[001]$ | $Ab_\gamma c_\beta Bc_\gamma$ | $T_\uparrow O:O$ | 4.38 | $\underline{Ab_\gamma c_\beta Bc_\alpha c_\gamma Ac_\beta}$ | $T_\uparrow O:OO:T_\uparrow$ | 0.00 | $Ab_\gamma c_\beta Bc_\alpha c_\gamma Ac_\beta b_\gamma Cb_\beta$ | $T_\uparrow O:OO:T_\uparrow O:O$ | 2.89 |
| $\kappa[001]$ | $\underline{Ac_\beta b_\gamma Cb_\alpha}$ | $T_\uparrow O:O$ | 0.14 | $Ac_\beta b_\gamma Cb_\alpha b_\beta Ac_\beta$ | $T_\uparrow O:OO:O$ | 3.22 | $Ac_\beta b_\gamma Cb_\alpha b_\beta Ab_\gamma c_\beta Bc_\alpha$ | $T_\uparrow O:OO:T_\uparrow O:O$ | 2.63 |
| $\kappa[001]$ | $\underline{Ac_\beta b_\gamma Cb_\beta}$ | $T_\uparrow O:O$ | 0.14 | $Ac_\beta b_\gamma Cb_\alpha b_\beta Ab_\gamma$ | $T_\uparrow O:OO:T_\uparrow$ | 0.60 | $Ac_\beta b_\gamma Cb_\alpha b_\beta Ab_\gamma c_\beta Bc_\gamma$ | $T_\uparrow O:OO:T_\uparrow O:O$ | 2.49 |
| $\kappa[001]$ | $Ac_\alpha c_\beta Ba_\beta$ | $OO:O$ | 2.43 | $Ac_\alpha c_\beta Bc_\gamma a_\beta Ca_\alpha$ | $OO:T_\uparrow O:O$ | 4.33 | $Ac_\alpha c_\beta Bc_\gamma a_\beta Ca_\alpha a_\gamma Bc_\gamma$ | $OO:T_\uparrow O:OO:O$ | 2.34 |
| $\kappa[001]$ | $Ac_\alpha c_\beta Bc_\gamma$ | $OO:T_\uparrow$ | 0.80 | $Ac_\alpha c_\beta Bc_\gamma a_\beta Ca_\gamma$ | $OO:T_\uparrow O:O$ | 5.05 | $Ac_\alpha c_\beta Bc_\gamma a_\beta Ca_\alpha a_\gamma Ba_\beta$ | $OO:T_\uparrow O:OO:T_\uparrow$ | 2.56 |
| $\kappa[001]$ | $Ab_\alpha b_\gamma Ca_\gamma$ | $OO:O$ | 2.20 | $Ab_\alpha b_\gamma Cb_\beta a_\gamma Ba_\alpha$ | $OO:T_\uparrow O:O$ | 3.86 | $Ab_\alpha b_\gamma Cb_\beta a_\gamma Ba_\alpha a_\beta Cb_\beta$ | $OO:T_\uparrow O:OO:O$ | 1.42 |
| $\kappa[001]$ | $\underline{Ab_\alpha b_\gamma Cb_\beta}\dagger$ | $OO:T_\uparrow$ | 0.00 | $Ab_\alpha b_\gamma Cb_\beta a_\gamma Ba_\beta$ | $OO:T_\uparrow O:O$ | 4.30 | $Ab_\alpha b_\gamma Cb_\beta a_\gamma Ba_\alpha a_\beta Ca_\gamma$ | $OO:T_\uparrow O:OO:T_\uparrow$ | 1.42 |
| $\kappa[00\bar{1}]$ | $Ac_\gamma a_\beta Ba_\gamma$ | $OT_\downarrow:O$ | 2.14 | $Ac_\gamma a_\beta Ba_\gamma a_\alpha Ca_\beta$ | $OT_\downarrow:OO:O$ | 3.15 | $\underline{Ac_\gamma a_\beta Ba_\gamma a_\alpha Ca_\beta c_\gamma Bc_\beta}$ | $OT_\downarrow:OO:T_\downarrow O:O$ | 0.62 |
| $\kappa[00\bar{1}]$ | $Ac_\gamma a_\beta Ba_\alpha$ | $OT_\downarrow:O$ | 1.64 | $Ac_\gamma a_\beta Ba_\gamma a_\alpha Cc_\gamma$ | $OT_\downarrow:OO:T_\downarrow$ | 2.25 | $\overline{Ac_\gamma a_\beta Ba_\gamma a_\alpha Ca_\beta c_\gamma Bc_\alpha}$ | $OT_\downarrow:OO:OT_\downarrow:O$ | 0.94 |
| $\kappa[00\bar{1}]$ | $Ab_\beta a_\gamma Ca_\beta$ | $OT_\downarrow:O$ | 2.15 | $Ab_\beta a_\gamma Ca_\beta a_\alpha Ba_\gamma$ | $OT_\downarrow:OO:O$ | 2.57 | $\underline{Ab_\beta a_\gamma Ca_\beta a_\alpha Ba_\gamma b_\beta Cb_\alpha}$ | $OT_\downarrow:OO:T_\downarrow O:O$ | 0.44 |
| $\kappa[00\bar{1}]$ | $Ab_\beta a_\gamma Ca_\alpha$ | $OT_\downarrow:O$ | 1.24 | $Ab_\beta a_\gamma Ca_\beta a_\alpha Bb_\beta$ | $OT_\downarrow:OO:T_\downarrow$ | 1.69 | $\overline{Ab_\beta a_\gamma Ca_\beta a_\alpha Ba_\gamma b_\beta Cb_\gamma}$ | $OT_\downarrow:OO:T_\downarrow O:O$ | 1.89 |
| $\kappa[00\bar{1}]$ | $Ac_\gamma c_\alpha Bb_\gamma$ | $OO:T_\downarrow$ | 2.36 | $Ac_\gamma c_\alpha Bc_\beta b_\gamma Ab_\alpha$ | $OO:OT_\downarrow:O$ | 1.67 | $\underline{Ac_\gamma c_\alpha Bc_\beta b_\gamma Ab_\beta b_\alpha Cb_\gamma}$ | $OO:OT_\downarrow:OO:O$ | 0.00 |
| $\kappa[00\bar{1}]$ | $Ac_\gamma c_\alpha Bc_\beta$ | $OO:O$ | 0.80 | $Ac_\gamma c_\alpha Bc_\beta b_\gamma Ab_\beta$ | $OO:OT_\downarrow:O$ | 4.84 | $\overline{Ac_\gamma c_\alpha Bc_\beta b_\gamma Ab_\beta b_\alpha Cc_\beta}$ | $OO:OT_\downarrow:OO:T_\downarrow$ | 4.62 |
| $\kappa[00\bar{1}]$ | $Ab_\beta b_\alpha Cc_\beta$ | $OO:T_\downarrow$ | 2.17 | $\underline{Ab_\beta b_\alpha Cb_\gamma c_\beta Ac_\alpha}$ | $OO:OT_\downarrow:O$ | 0.37 | $Ab_\beta b_\alpha Cb_\gamma c_\beta Ac_\gamma c_\alpha Bc_\beta$ | $OO:OT_\downarrow:OO:O$ | 3.81 |
| $\kappa[00\bar{1}]$ | $\underline{Ab_\beta b_\alpha Cb_\gamma}\dagger$ | $OO:O$ | 0.00 | $\overline{Ab_\beta b_\alpha Cb_\gamma c_\beta Ac_\gamma}$ | $OO:OT_\downarrow:O$ | 3.91 | $Ab_\beta b_\alpha Cb_\gamma c_\beta Ac_\gamma c_\alpha Bb_\gamma$ | $OO:OT_\downarrow:OO:T_\downarrow$ | 3.91 |

**Table 2.** Stacking sequence and Al coordination of *unrelaxed* alumina films with $Al_{4n-2}O_{6n}$ stoichiometry and their relative total-energy differences $E_{rel}$ *after* relaxation. Notation and grouping are the same as in Tab. 1. Configurations that differ only in their surface Al ion are grouped together and separated by larger whitespace. The coordination given for the surface Al ion is the one that it would have in the bulk. The *ab initio* study and comparison permit us to make the following set of observations: (i) Although the stable films are generally of $\kappa$ type, $\alpha$-type films are competitive, at least for the thinnest films; (ii) For the thinner films, both $\kappa[001]$ and $\kappa[00\bar{1}]$ orientations yield stable and metastable configurations, while for the thicker films, only $\kappa[00\bar{1}]$ leads to (meta-)stable configurations; (iii) The general trend in stability with respect to the O stacking is the same as for the $Al_{4n-4}O_{6n}$ films ($AC$ more favorable than $AB$) but with exceptions, in particular, the stable $Al_{10}O_{18}$ and $Al_{14}O_{24}$ configurations originate from structures with $AB$ stacking in the first two O layers.

| alumina group | $Al_8O_{12}$ films: alumina stacking | coord. of Al ions | $E_{rel}$ (eV/cell) | $Al_{12}O_{18}$ films: alumina stacking | coord. of Al ions | $E_{rel}$ (eV/cell) |
|---|---|---|---|---|---|---|
| $\alpha$ | $Ac_3c_2Bc_1c_3$ | $OO:OO$ | 2.46 | $Ac_3c_2Bc_1c_3Ac_2c_1$ | $OO:OO:OO$ | 2.88 |
| $\alpha$ | $Ab_2b_3Cb_1b_2$ | $OO:OO$ | 1.92 | $Ab_2b_3Cb_1b_2Ab_3b_1$ | $OO:OO:OO$ | 3.93 |
| $\kappa[001]$ | $Ab_\gamma c_\beta Bc_\alpha c_\gamma$ | $T_\uparrow O:OO$ | 3.17 | $Ab_\gamma c_\beta Bc_\alpha c_\gamma Ac_\beta b_\gamma$ | $T_\uparrow O:OO:T_\uparrow O$ | 1.42 |
| $\kappa[001]$ | $Ac_\beta b_\gamma Cb_\alpha b_\beta$ | $T_\uparrow O:OO$ | 2.57 | $Ac_\beta b_\gamma Cb_\alpha b_\beta Ab_\gamma c_\beta$ | $T_\uparrow O:OO:T_\uparrow O$ | 1.16 |
| $\kappa[001]$ | $Ac_\alpha c_\beta Bc_\gamma a_\beta$ | $OO:T_\uparrow O$ | 4.07 | $Ac_\alpha c_\beta Bc_\gamma a_\beta Ca_\alpha a_\gamma$ | $OO:T_\uparrow O:OO$ | 2.78 |
| $\kappa[001]$ | $Ab_\alpha b_\gamma Cb_\beta a_\gamma$ | $OO:T_\uparrow O$ | 2.06 | $Ab_\alpha b_\gamma Cb_\beta a_\gamma Ba_\alpha a_\beta$ | $OO:T_\uparrow O:OO$ | 1.48 |
| $\kappa[00\bar{1}]$ | $Ac_\gamma a_\beta Ba_\gamma a_\alpha$ | $OT_\downarrow:OO$ | 2.08 | $Ac_\gamma a_\beta Ba_\gamma a_\alpha Ca_\beta c_\gamma$ | $OT_\downarrow:OO:OT_\downarrow$ | 0.49 |
| $\kappa[00\bar{1}]$ | $Ab_\beta a_\gamma Ca_\alpha a_\beta$ | $OT_\downarrow:OO$ | 0.00 | $Ab_\beta a_\gamma Ca_\beta a_\alpha Ba_\gamma b_\beta$ | $OT_\downarrow:OO:OT_\downarrow$ | 0.00 |
| $\kappa[00\bar{1}]$ | $Ac_\gamma c_\alpha Bc_\beta b_\gamma$ | $OO:OT_\downarrow$ | 2.90 | $Ac_\gamma c_\alpha Bc_\beta b_\gamma Ab_\beta b_\alpha$ | $OO:OT_\downarrow:OO$ | 1.72 |
| $\kappa[00\bar{1}]$ | $Ab_\beta b_\alpha Cb_\gamma c_\beta$ | $OO:OT_\downarrow$ | 1.80 | $Ab_\beta b_\alpha Cb_\gamma c_\beta Ac_\gamma c_\alpha$ | $OO:OT_\downarrow:OO$ | 0.52 |

**Table 3.** Stacking sequence and Al coordination of the *unrelaxed* alumina films with $Al_{4n}O_{6n}$ stoichiometry and their relative total-energy differences $E_{rel}$ *after* relaxation. Notation and grouping are the same as in Tab. 1. The *ab initio* study and comparison permit a number of observations that are similar to those we made for the $Al_{4n-4}O_{6n}$ films (Tab. 1).

## 2. Supplementary material for Section 5.1.

Tables 1, 2, and 3 list the stacking sequences of all unrelaxed thin-film candidates. Apart from the detailed stacking, we also characterize the films in terms of the distribution of octahedrally ($O$) and tetrahedrally ($T_\downarrow$ and $T_\uparrow$ for tetrahedra pointing towards and away from the substrate) coordinated Al ions and in terms of the interfacial orientations $\alpha = \mathrm{TiC}[111]/\alpha[001]$ ($\Leftrightarrow \mathrm{TiC}[111]/\alpha[00\bar{1}]$), $\kappa[001] = \mathrm{TiC}[111]/\kappa[001]$, and $\kappa[00\bar{1}] = \mathrm{TiC}[111]/\kappa[00\bar{1}]$) [1]. Finally, we also list the relative energy for each relaxed film geometry. The relative energy is defined as $E_{\mathrm{rel}} = E - E_0$, where $E$ is the total system under consideration and $E_0$ the total energy of the energetically most favorable system with the same stoichiometric composition. The low-energy configurations (stable or metastable in the sense defined in the research paper) are highlighted (underlined) in the tables.

In the following we give a more detailed account of the trends in phase content, orientation, and preferred stacking, Section V.A. in the research paper:

A thorough inspection of tables 1, 2, and 3 shows that, as a general trend, the stable and metastable alumina films are obtained upon relaxing TiC/thin-film-alumina geometries with initial orientation $\mathrm{TiC}/\kappa\text{-}\mathrm{Al_2O_3}[00\bar{1}]$. In particular the preferation over $\mathrm{TiC}/\alpha$ configurations is in agreement with the experimental observation that growth of $\kappa\text{-}\mathrm{Al_2O_3}$ is preferred over $\alpha\text{-}\mathrm{Al_2O_3}$ on TiC(111) [2]. However, relaxation of initial $\mathrm{TiC}/\alpha\text{-}\mathrm{Al_2O_3}$ and $\mathrm{TiC}/\kappa\text{-}\mathrm{Al_2O_3}[001]$ configurations yields (meta-)stable in the case of the thinner films ($n = 2, 3$ O layers) in the case of $\mathrm{Al}_{4n-2}\mathrm{O}_{6n}$ stoichiometry.

Comparing the energetics of configurations that differ only by a reflecting the alumina film about the $yz$-plane, we notice that, generally, the unrelaxed geometries with an $AC$ stacking in the bottom two O layers become more favorable upon relaxation than the ones with an $AB$ stacking. There are, however, exceptions; in particular the energetically most favorable $\mathrm{Al_{10}O_{18}}$ film and each one of the potentially metastable $\mathrm{Al_{10}O_{18}}$ and $\mathrm{Al_{14}O_{24}}$ films posses an $AB$ stacking in the bottom two O layers. We also note that the highlighted films for a fixed stoichiometry, that is $\mathrm{Al}_{4n-4}\mathrm{O}_{6n}$, $\mathrm{Al}_{4n-2}\mathrm{O}_{6n}$ , or $\mathrm{Al}_{4n}\mathrm{O}_{6n}$, but with varying thickness ($n$), do in general not lie in the same row of the table. Thus, the details of the stacking sequence at the interface of the films that result into the low-energy energy configurations varies strongly with the film thickness (since configurations that do lie within one such row possess the same stacking at the interface and differ only in their thickness).

In summary, although there are some general stability trends that can be inferred from the phase content, orientation, and stacking of the unrelaxed thin-film configurations, there are also several noticeable exceptions. In particular the $\mathrm{Al}_{4n-2}\mathrm{O}_{6n}$ films tend to break the rules. The observation of such exception demonstrates the potential danger of applying simple Monte Carlo methods with importance sampling based on a classification in terms of for example unrelaxed stacking, phase content, and/or orientation, since important exceptions may easily be missed.

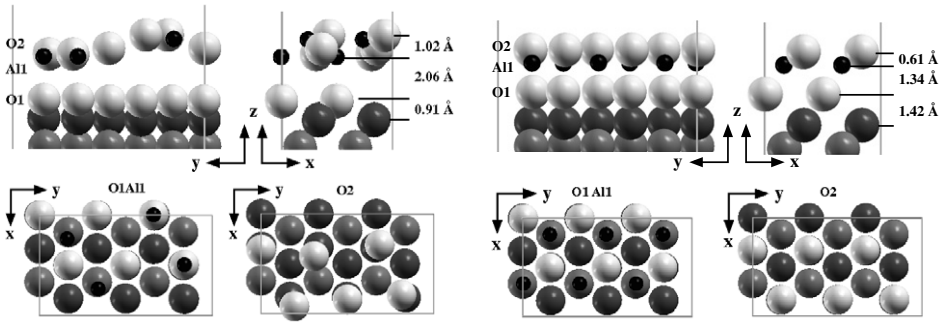


**Figure 1.** Atomic structure of the stable $Al_4O_{12}$ (left column) and $Al_6O_{12}$ films (right column). The top panels show the projected side views along [100] and [010] including interlayer distances. The bottom panels show the top views on the atomic layers [as defined in the top panels]. Color coding and notation: Dark gray = Ti, light gray = C, light = O, and black = Al; *O*: octahedrally coordinated Al, *T*: tetrahedrally coordinated Al, the arrow indicates the direction in which the tetrahedra point. We notice large O–O interlayer separation in the $Al_4O_{12}$ film which results into an almost empty region in between the two O layers (top left panel). As a consequence, the TiC/alumina system separates into TiC/O/alumina. The Al coordination is $T_{\downarrow}O$ (bottom left panel). The $Al_6O_{12}$ film forms a close-packed structure with an O-terminated surface (top right panel). The stronger TiC/$Al_6O_{12}$ binding is evident. All Al ions are octahedrally coordinated (bottom right panel).

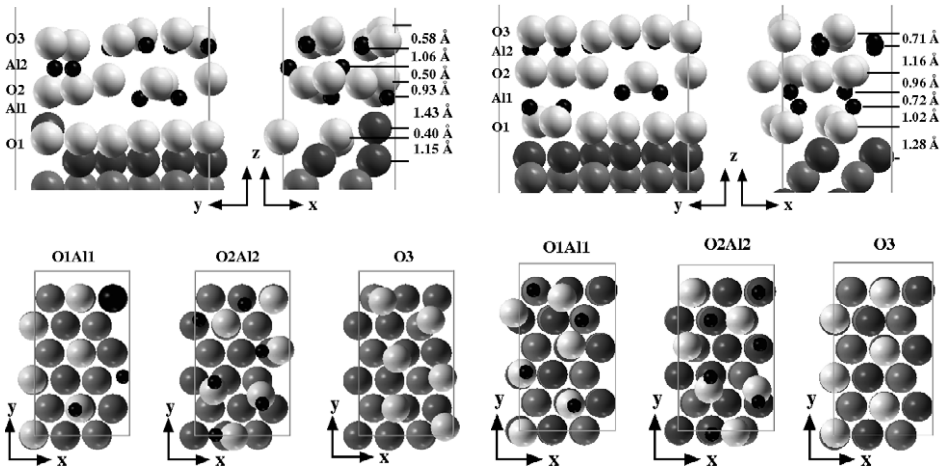


**Figure 2.** Atomic structure of the stable $Al_8O_{18}$ (left column) and $Al_{10}O_{18}$ film (right column). Color coding and notation as in figure 1. We notice that one of interfacial Ti atoms has relaxed to a position slightly above the bottom O layer in the $Al_8O_{18}$ film (top right panel). This Ti impurity may considerably strengthen the TiC–alumina bond. In the top view on O1Al1 (bottom right panel), this Ti impurity is indicated by the large black ball. The Al coordination is $T_{\downarrow} : OT_{\downarrow}T_{\downarrow}$. The $Al_{10}O_{18}$ is less distorted (top right panel). The surface is O terminated after relaxation. The Al coordination is $T_{\downarrow}T_{\uparrow} : T_{\downarrow}OO$ (bottom right panel). We emphasize that tetrahedral coordination dominates and that the tetrahedra associated with both Al pairs in the bottom layer are pointing in opposite directions ($T_{\uparrow}T_{\downarrow}$).

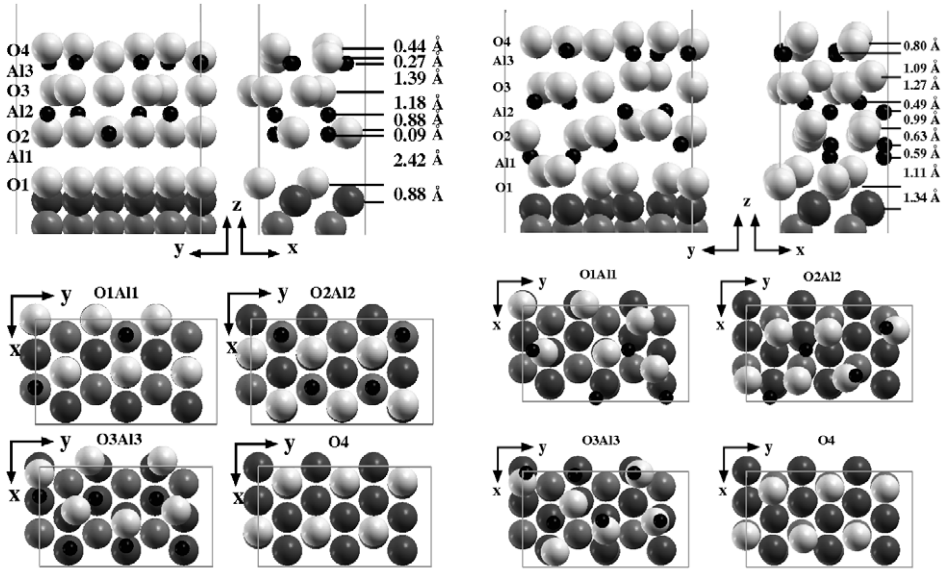


**Figure 3.** Atomic structure of the stable $Al_{12}O_{24}$ (left column) $Al_{14}O_{24}$ films (right column). Color coding and notation as in figure 1. We notice again the large interlayer distance between the bottom two O layers in the $Al_{12}O_{24}$ film (top left panel), showing that the TiC/alumina system separates into weakly bound TiC/O/alumina. The Al coordination is $O : OO : OOO$, *i.e.*, purely octahedral (bottom left panel). The stronger binding or the $Al_{14}O_{24}$ film to the substrate is evident (top right panel). The surface is O terminated. The Al coordination is $OT_{\downarrow} : T_{\uparrow}T_{\downarrow} : OT_{\downarrow}T_{\downarrow}$ (bottom right panel). We notice that the tetrahedra associated with the two Al ions in the second layer point into opposite directions ($T_{\downarrow}T_{\uparrow}$).

## 3. Supplementary material for Section 5.3. and 5.5.

Figures 1 through 4 may facilitate the identification of the occupied stacking sites and the coordinations of individual atoms/layers in the low-energy $Al_{4n-2}O_{6n}$ and $Al_{4n-4}O_{6n}$ thin-film configurations that are discussed in great detail in the research paper. In addition to the side views on the stable and metastable thin-film geometries that are already presented in the research paper, we here include also top views on every single atomic layer.

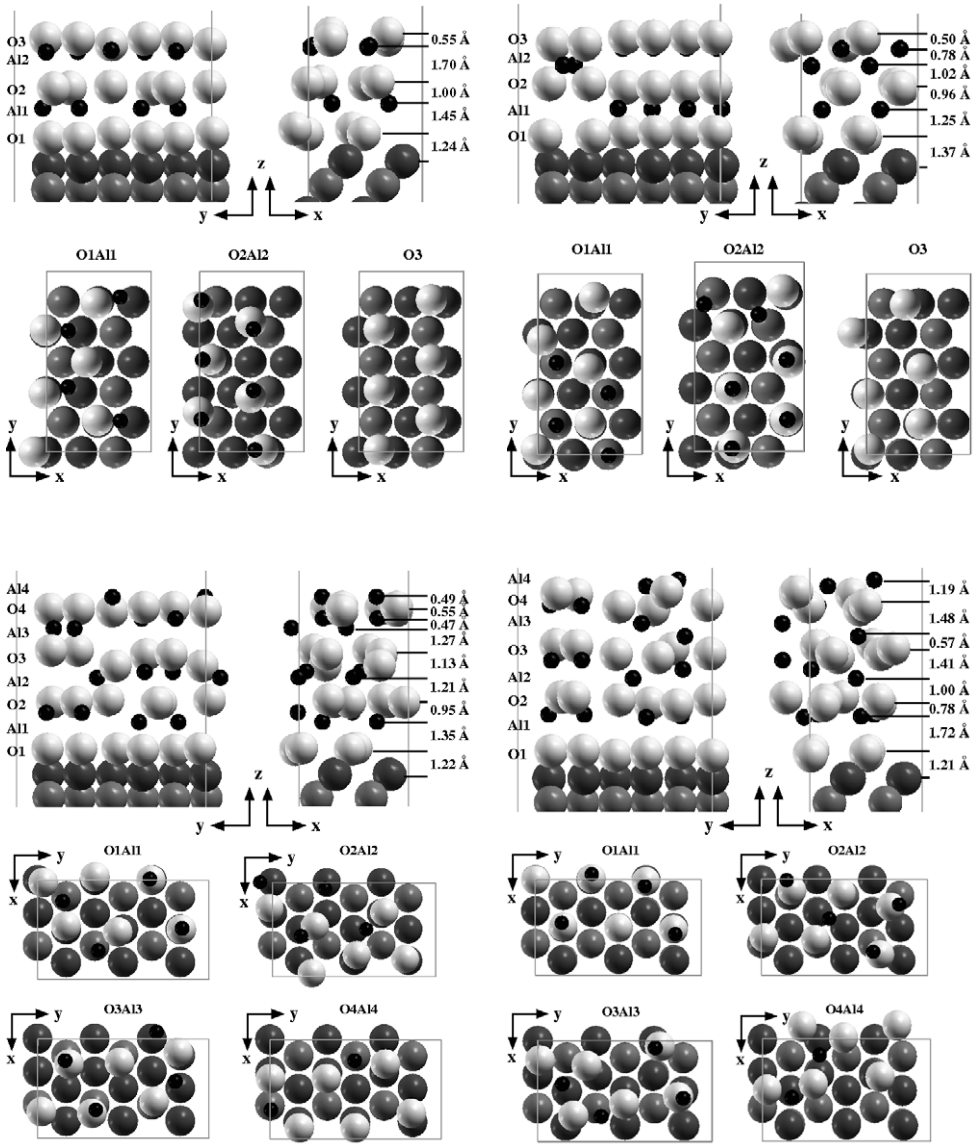


**Figure 4.** Atomic structure of the potentially metastable $Al_{10}O_{18}$ (top two groups of panels) and $Al_{14}O_{24}$ films (bottom two groups of panels). Color coding and notation are as in figure 1. In the $Al_{10}O_{18}$ films the Al coordinations are $OO : T_{\downarrow}T_{\downarrow}T_{\downarrow}$ and $OO : T_{\downarrow}T_{\downarrow}O$. The $Al_{14}O_{24}$ films are Al terminated even after relaxations. The Al coordinations are (without surface Al) $OT_{\downarrow} : OO : T_{\downarrow}O$, $T_{\downarrow}T_{\downarrow} : T_{\downarrow}(t_{\downarrow}o) : T_{\downarrow}O$ ($t$ single tetrahedral Al ion, $o$ single octahedral Al ion).

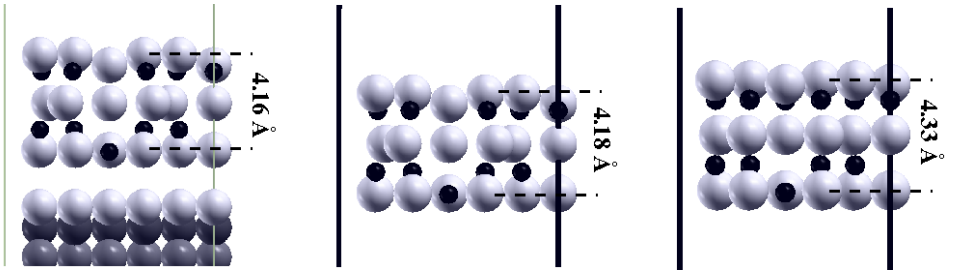


**Figure 5.** Side views of $Al_{4(n-1)}O_{6(n-1)}$ overlayers along [010] in the presence of the oxygen passivated TiC/O substrate (left panel), obtained by removing the substrate, but keeping the substrate lattice parameter and allowing for further relaxations (mid-panel) , and after adjusting the lattice parameter to that of $\alpha$-$Al_2O_3$ and letting the atoms relax (right panel) . Apart from the different thicknesses and some minor differences in the relative positions of a few O atoms, all three geometries are essentially identical. Thus, their chemical, that is, binding properties, are essentially the same. In summary, the TiC/O-alumina binding is extremely weak in the $Al_{4n-4}O_{6n}$ forms and the anchoring cannot be expected to be significantly enhanced due to expected relaxations in an improved model that permits incommensurate lattices of the stoichiometric overlayer and the TiC/O substrate.

## 4. Supplementary material for Section 5.4.

In general, the TiC/$Al_{4n-4}O_{6n}$ configurations separate into a O passivated TiC/O substrate and a fully stoichiometric $Al_{4(n-1)}O_{6(n-1)}$ overlayer. Here we give the details that show that the overlayer only exhibits an extremely weak binding to the substrate, and that the lattice mismatch between the substrate and the overlayer does not have an effect on the structure or on the anchoring.

We have performed calculations for the the lowest-energy TiC/$Al_{4n-4}O_{6n}$ system ($n = 4$), (i) where we remove the substrate, but keep the lattice constant fixed, and allow for further relaxations, and (ii) where we also adjust the lattice parameter to that of $\alpha$-$Al_2O_3$.

Figure 5 shows that neither the substrate, nor the value of the lattice parameter influence the atomic structure in a significant way. In fact, removing the substrate has hardly any consequences, which shows how extremely weak the interaction between the TiC/O and the alumina overlayer is. Adjusting the lattice parameter to that of $\alpha$-$Al_2O_3$(decreasing by $\sim$10%) only results in an adjustment of the film thickness (increasing, as expected). We conclude that the chemical properties, in particular the binding of the film can not be expected to change due to relaxations of an incommensurate stoichiometric overlayer.

## References

[1] We note that for films with orientation TiC[111]/$\kappa$[001], the tetrahedra associated with tetrahedrally coordinated Al ions always point upward, that is, away from the substrate. Correspondingly, for films with orientation TiC[111]/$\kappa$[001], the tetrahedra point downward, that is, towards the substrate.

[2] M. Halvarsson, H. Nordén, and S. Vuorinen, Surf. Coat. Technol. **61**, 177 (1993).